Lens distortion correction with a calibration harp

4 authors, including:

Pascal Monasse
Université Paris-Est Marne-la-Vallée
92 PUBLICATIONS   **1,452** CITATIONS

SEE PROFILE

Zhongwei Tang
Huawei Technologies
14 PUBLICATIONS   **153** CITATIONS

SEE PROFILE

Some of the authors of this publication are also working on these related projects:

Project   Image restoration View project

LENS DISTORTION CORRECTION WITH A CALIBRATION HARP

R. Grompone von Gioi,[†] *P. Monasse,*[‡] *J.-M. Morel,*[†] *and Z. Tang*[†]

[†]CMLA, ENS-Cachan, France   [‡]IMAGINE, LIGM-Université Paris Est, France

ABSTRACT

Plumb line lens distortion correction methods permit to avoid numerical compensation between the camera internal and external parameters in global calibration method. Once the distortion has been corrected by a plumb line method, the camera is ensured to transform, up to the distortion precision, 3D straight lines into 2D straight lines, and therefore becomes a pinhole camera. This paper introduces a plumb line method for correcting and evaluating camera lens distortion with high precision. The evaluation criterion is defined as the average standard deviation from straightness of a set of approximately equally spaced straight strings photographed uniformly in all directions by the camera, so that their image crosses the whole camera field. The method uses an easily built "calibration harp," namely a frame on which good quality strings have been tightly stretched to ensure a very high physical straightness. Real experiments confirm that our method produces high precision corrections (less than 0.05 pixel), approximating the distortion with a large number of degrees of freedom given by a polynomial model of order eleven.

Index Terms— Lens distortion, error compensation, plumb lines, polynomial model.

1. INTRODUCTION

This paper presents a method to correct camera lens distortion with high precision. By high precision, we mean deviations from straightness of about 0.1 pixel for a straight line crossing the whole camera field. Such a precision is hardly appreciable for a human observer. However, there is no limit to the desired precision when the camera is used for 3D reconstruction or photogrammetry tasks. Traditionally, lens distortion and the other camera parameters are estimated simultaneously as camera internal and external parameters [1, 2, 3, 4, 5]. In these global calibration methods all parameters are estimated by minimizing the error between the camera and its numerical model on feature points identified in several views, all in a single non-linear optimization. The result will be precise if (and only if) the model captures the correct physical properties of cameras and if the minimization algorithm finds a global minimum. Unfortunately, global camera calibration suffers a common drawback: errors in the external and internal camera parameter can be compensated by opposite errors in the distortion model. Thus the residual error can be apparently small, while the distortion model is not precisely estimated [5, 6]. For example, the Lavest et al. method [4] measures the non-flatness of a pattern and yields a remarkably small re-projection error of about 0.02 pixels, while the straightness of corrected lines has a 0.2 pixel RMSE. Fortunately the error compensation in global calibration can be avoided by proceeding to distortion correction before camera calibration. Recent distortion correction methods use the correspondences between two or several images, without knowledge of any camera information. The main tool they use is slackened epipolar constraints, which incorporate lens distortion into the epipolar geometry. Several iterative [7, 8] or non-iterative methods [9, 10, 11, 6, 12] are used to estimate the distortion and to correct it. These methods are used with a low order parametric distortion model and therefore cannot achieve high precision.

Non-parametric methods which establish a direct diffeomorphism between a flat pattern and a frontal photograph of it [13, 14] should be ideal for high precision distortion correction. Indeed, they do not depend on the *a priori* choice of a distortion model with a fixed number of parameters. Yet to achieve a high precision, they depend on the design of a very flat non deformable plate with highly accurate patterns printed on it.[1] This replaces a technological challenge by another, which is not simpler. Plumb-line methods [15] should therefore be an alternative because, as we shall see, it is easier to create very straight lines. For plumb-line methods, a distortion model is still necessary to precisely remove the distortion, and most existing models can be used. Nevertheless, some of them are too complicated [15], while some are not general enough to capture the distortion [16]. For most distortion models, the distortion center is a sensitive parameter when a realistic distortion is treated. The barely polynomial approximation proposed in [17] is therefore a good choice, being a translation invariant and linear approximation of any vector field. This model-free formulation can approximate complex radial and non-radial distortions as well, provided the polynomial degree is high enough. According to the criteria of *self-consistency* and *universality*[2] developed in [17] to compare many camera distortion models, the polynomial models are the most flexible and accurate.

---

[1]A 10 micron flatness could be needed to achieve a precision of 0.01 pixels.

[2]Self-consistency is evaluated by the residual error when distortion generated with a certain model is corrected (using the model in reverse way) by the best parameters for the same model. Analogously, universality is measured by the residual error when a model is used to correct distortions generated by a family of other models. A model is self-consistent and universal if it can approximate any other model and the inverse of any other model, including itself, with the desired precision. Polynomials of order 11 are 0.01 pixels self-consistent and universal.

The proposed method is introduced in section 2, followed by real experiments in section 3, along with a comparison to a non-parametric method. Section 4 concludes the paper.

2. THE HARP CALIBRATION METHOD

In one sentence, the proposed method combines the advantage of plumb-line methods with the universality of the polynomial approximation. The plumb-line method consists in correcting the distorted points which are supposed to be on a straight line, by minimizing the average squared distance from the corrected points to their corresponding regression lines.

The polynomial model has the form

$$
\begin{aligned}
x_u &= b_0 x_d^p + b_1 x_d^{p-1} y_d + b_2 x_d^{p-2} y_d^2 + \cdots + b_p y_d^p \\
&\quad + b_{p+1} x_d^{p-1} + b_{p+2} x_d^{p-2} y_d + \cdots + b_{2p} y_d^{p-1} \\
&\quad + \cdots + b_{\frac{(p+1)(p+2)}{2}-3} x_d + b_{\frac{(p+1)(p+2)}{2}-2} y_d \\
&\quad + b_{\frac{(p+1)(p+2)}{2}-1} \\
y_u &= c_0 x_d^q + c_1 x_d^{q-1} y_d + c_2 x_d^{q-2} y_d^2 + \cdots + c_q y_d^q \\
&\quad + c_{q+1} x_d^{q-1} + c_{q+2} x_d^{q-2} y_d + \cdots + c_{2q} y_d^{q-1} \\
&\quad + \cdots + c_{\frac{(q+1)(q+2)}{2}-3} x_d + c_{\frac{(q+1)(q+2)}{2}-2} y_d \\
&\quad + c_{\frac{(q+1)(q+2)}{2}-1}
\end{aligned} \tag{1}
$$

with (x_u, y_u) undistorted point and (x_d, y_d) distorted point. The polynomial approximation being translation invariant, the origin is arbitrarily fixed at the image center. The order for the x and y components is respectively p and q. The number of parameters for x and y is respectively $\frac{(p+1)(p+2)}{2}$ and $\frac{(q+1)(q+2)}{2}$. The model is called bicubic model when $p = q = 3$.

In the following, we show how to integrate the polynomial model into the plumb-line method. Given a set of corrected points $(x_{u_i}, y_{u_i})_{i=1,\cdots,N}$ which are supposed to be on a line, the first step is to compute the linear regression line

$$
\alpha x_{u_i} + \beta y_{u_i} - \gamma = 0 \tag{2}
$$

with $\alpha = \sin\theta$, $\beta = \cos\theta$, $\tan 2\theta = -\frac{2(A_{xy} - A_x A_y)}{V_{xx} - V_{yy}}$, $A_x = \frac{1}{N}\sum_{i=1}^{N} x_{u_i}$, $A_y = \frac{1}{N}\sum_{i=1}^{N} y_{u_i}$, $A_{xy} = \frac{1}{N}\sum_{i=1}^{N} x_{u_i} y_{u_i}$, $V_{xx} = \frac{1}{N}\sum_{i=1}^{N}(x_{u_i} - A_x)^2$, $V_{yy} = \frac{1}{N}\sum_{i=1}^{N}(y_{u_i} - A_y)^2$, and $\gamma = A_x \sin\theta + A_y \cos\theta$. The sum of squared distances from the points to this regression line is $\sum_{i=1}^{N}(\alpha x_{u_i} + \beta y_{u_i} - \gamma)^2$. By considering G groups of lines, the total sum of squared distance is

$$
S = \sum_{g=1}^{G} \sum_{l=1}^{L_g} \sum_{i=1}^{N_{gl}} (\alpha_g x_{u_{gli}} + \beta_g y_{u_{gli}} - \gamma_{gl})^2 \tag{3}
$$

with L_g the number of lines in group g, and N_{gl} the number of points of line l in group g. Given the total number of points

$N = \sum_{g=1}^{G} \sum_{l=1}^{L_g} N_{gl}$, the root mean squared distance (RMS error) is defined by

$$
d = \sqrt{\frac{S}{N}}. \tag{4}
$$

For a sake of succinctness, the following discussion will assume a bicubic model with $p = q = 3$. Combining Eq. (1) and Eq. (3), the energy S becomes

$$
\begin{aligned}
S &= \sum_{g=1}^{G} \sum_{l=1}^{L_g} \sum_{i=1}^{N_{gl}} \Big(\alpha_g \big(b_0 x_{d_{gli}}^3 + \cdots + b_9 \big) \\
&\quad + \beta_g \big(c_0 x_{d_{gli}}^3 + \cdots + c_9 \big) - \gamma_{gl} \Big)^2.
\end{aligned} \tag{5}
$$

It is a non-linear problem to minimize the energy S with respect to the parameters $b_0, \cdots, b_9, c_0, \cdots, c_9$. But the problem becomes linear by assuming that the orientation parameters α_g, β_g are known. By differentiating S with respect to each parameter, we obtain a linear system

$$
\mathbf{A}\mathbf{x} = \mathbf{0} \tag{6}
$$

with $\mathbf{x} = (b_0, \cdots, b_9, c_0, \cdots, c_9, \gamma_{11}, \cdots, \gamma_{GL_G})^T$ and the coefficient matrix $\mathbf{A}$. To obtain a unique non-trivial solution, we always set $b_7 = c_8 = 1$, $b_9 = c_9 = 0$, which in fact fixes a scale and a translation to the solution. The minimized S can be changed by the introduced scale. But this change is consistent if the distortion center and b_9, c_9, b_7, c_8 are fixed.

In practice, the orientation of lines is unknown and the minimization of the energy in Eq. (5) is a non-linear problem. The minimization is performed by first doing an iterative Levenberg-Marquardt (LM) algorithm which estimates the parameters of polynomials of increasing order. The algorithm starts estimating the parameters of a 3-order polynomial; the result is used to initialize the 4-order polynomial, and the process continues until 11-order. After this first step, the linear estimation in Eq. (6) is performed iteratively to refine the precision. The line orientations are first initialized by the orientation of the regression lines obtained by the LM method, and then with the values of the previous linear step. The iteration is repeated until the results stabilize or the required precision is reached.

3. EXPERIMENTS

In this section, we describe real experiments with a strong distortion comparing the proposed method with a non-parametric flat pattern-based method [13].

The experiments were made with a Canon EOS 30D reflex camera with EFS $18 - 55$mm lens. The minimal focal length (18mm) was chosen to produce a fairly large distortion. The RAW images were demosaicked by summing up the four pixels of each 2×2 Bayer cell, obtaining a half-size image. The calibration harp was built by tightly stretching good quality strings on a frame to ensure a very high physical straightness (our calibration harp was built with sewings

string). The high distortion is visible near the border of the image (see the images in Fig. 1 for example). On each corrected line, sub-pixel precise edge points were obtained by Devernay's algorithm [18] and then groupped when belonging to the same line segments detected by the LSD algorithm [19]. 18 photographs of the calibration harp with different orientations (some of them in Fig. 1) were used in the calibration by the 11-degree polynomial model. Independent distorted images (for example, see the top image in Fig. 2) are used for verification. The correction result is recapitulated in Fig. 2. The non-parametric pattern-based method in [13] was also tried (see result in Fig. 3), which estimates the distortion as the diffeomorphism (up to a homography) mapping the original digital pattern to a photograph of it by triangulating and interpolating dense correspondences. Note that in Fig. 2 and 3, y-axis has the same range, from -0.3 pixels to 0.3 pixels.

For the non-parametric method, a global tendency in the straightness error of the corrected lines can be observed (see Fig. 3). This was in fact due to the unavoidable drawback of this method: there is never a guarantee that the pattern is completely flat. The non-flatness of the pattern introduces a bias in the estimated distortion field, which causes the observable global residual in the curves plotted in Fig. 3. To eliminate this error source, the solution is either to construct a very flat pattern, or to recover the 3D shape of a non-flat pattern. Both are not really feasible. Yet, to appropriately use a plumb-line method, we need a pattern containing very straight lines, and this is far easier in practice. As shown in Fig. 2, the distortion correction is so accurate that no visible global tendency is visible in the corrected curves. The root mean square (RMS) distance of each line is also significantly smaller than for the non-parametric method (Table 1). It is particularly striking in Fig. 2 that the superimposed curves of the left and right side of each string are fairly uncorrelated, meaning that no deterministic distortion is left. The erratic oscillation of very small amplitude can be attributed to any cause, from the lack of the uniformity of the harp background causing a shift in the edge detection, to aliasing in the image itself. But it cannot be due to a residual mismatch of the polynomial model itself, because otherwise the curves on both sides of each string would be parallel. This confirms *a posteriori* the reliability of the polynomial model.

4. CONCLUSION

By combining the advantages of a model-free polynomial approximation and of a real plumb line pattern, the proposed lens distortion correction is significantly more accurate than parametric methods on flat patterns. The "calibration harp" construction only requires the acquisition of a string with decent quality. It is far simpler than realizing a flat plate with highly accurate patterns engraved on it. (The calibration of such patterns is not easier than lens calibration itself!) The high number of degrees of freedom in the unstructured model

line No.	RMSE (in pixels)	
	proposed method	non-parametric [13]
1	0.046 / 0.036	0.048 / 0.042
2	0.050 / 0.068	0.088 / 0.082
3	0.057 / 0.054	0.166 / 0.168
4	0.051 / 0.073	0.135 / 0.126
5	0.061 / 0.076	0.082 / 0.080
6	0.052 / 0.056	0.069 / 0.062
7	0.039 / 0.017	0.095 / 0.080
8	0.042 / 0.054	0.133 / 0.143
9	0.035 / 0.036	0.154 / 0.162

Table 1: RMS Error from edge points of corrected lines to their corresponding regression line. The proposed method is compared to non-parametric pattern-based method [13]. Each cell in the table contains two values, one for each side of the string. The lines are numerated in the top image in Fig. 2.

explains why we can call the method model-free. The only assumption on the lens distortion is its smoothness, implying that a polynomial with high enough order approximates it. In our experiments, the approximation error stabilizes for polynomials of degree 7 to 11. It might be objected that the high number of parameters in the polynomial interpolation (156 for an 11-order polynomial) could cause some bias in the result. Yet, the number of control points is far higher: There were about 10 strings for each orientation, some 30 control points on each string side, and some 18 orientations. Thus the number of control points is about 10000 and therefore 60 times more than the number of polynomial coefficients. A visual examination of the two sides of the strings confirms that no artificial simultaneous bias has been introduced by the polynomial distortion correction. This observation seems to indicate that most of the 0.05 pixels remaining oscillation is due either to image processing factors, or to background inhomogeneity, to aliasing in the edge detector, or to string diameter variations. It is not easy to decide which factor is dominant. Future work will concentrate on the precision of external camera calibration, and eventually on the 3D precision after having removed the lens distortion by the present
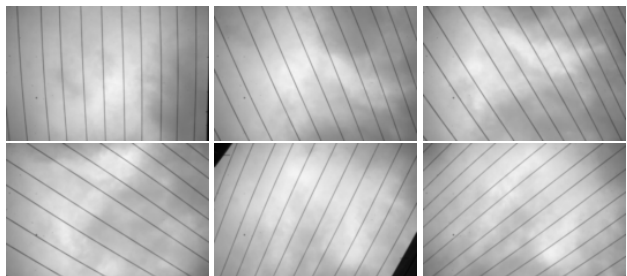

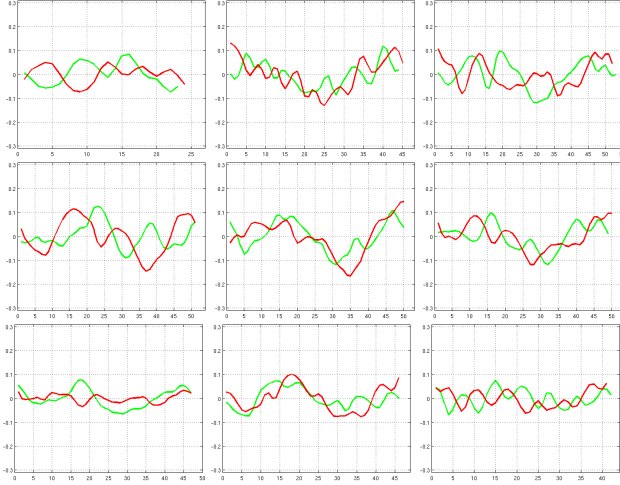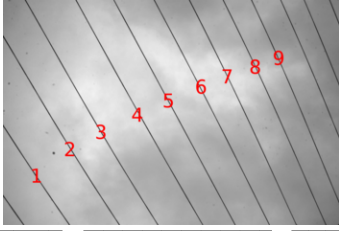**Fig. 1**: Six of the 18 photos of "calibration harp" with different orientation.

Fig. 2: Correction performance of the proposed method. Top row, the independent distorted image. The lines are numerated in red. From the second row to the last row, from left to right: the distance from the edge point of corrected lines to their corresponding regression line. Note that each figure contains two curves because there are two lines for one string. The range of y-axis is from -0.3 pixels to 0.3 pixels.
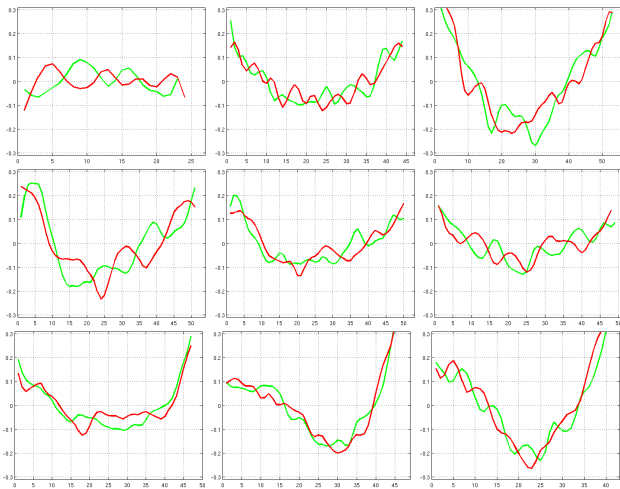

Fig. 3: Correction performance of non-parametric pattern-based method [13]. See the caption of Fig. 2 for details.

method.

5. REFERENCES

[1] C. C Slama, *Manual of Photogrammetry, 4th edition*, Falls Church, American Society of Photogrammetry, Virginia, 1980.

[2] Roger Y. Tsai, "A versatile camera calibration technique for high-accuracy 3D machine vision metrology using off-the-shelf tv cameras and lenses," *IEEE Journal of Robotics and Automation*, vol. Vol. RA-3, 1987.

[3] Z. Zhang, "A flexible new technique for camera calibration," *ICCV*, pp. 663–673, Sept. 1999.

[4] J. Lavest, M. Viala, and M. Dhome, "Do we really need accurate calibration pattern to achieve a reliable camera calibration?," *ECCV*, vol. 1, pp. 158–174, 1998.

[5] J. Weng, P. Cohen, and M. Herniou, "Camera calibration with distortion models and accuracy evaluation," *TPAMI*, vol. 14(10), pp. 965–980, 1992.

[6] H. Li and R. Hartley, "A non-iterative method for correcting lens distortion from nine point correspondences," *OmniVis*, 2005.

[7] Gideon P. Stein, "Lens distortion calibration using point correspondences," *CVPR*, p. 602608, 1997.

[8] Z. Zhang, "On the epipolar geometry between two images with lens distortion," *ICPR*, pp. 407–411, 1996.

[9] T. Pajdla and B. Micusik, "Estimation of omnidirectional camera model from epipolar geometry," *CVPR*, pp. 485–490, 2003.

[10] A. W. Fitzgibbon, "Simultaneous linear estimation of multiple view geometry and lens distortion," *CVPR*, vol. 1, pp. 125–132, 2001.

[11] J.P. Barreto and K. Daniilidis, "Fundamental matrix for cameras with radial distortion," *ICCV*, vol. 1, pp. 625632, 2005.

[12] D. Claus and A.W. Fitzgibbon, "A rational function lens distortion model for general cameras," *CVPR*, vol. 1, pp. 213–219, 2005.

[13] R. Grompone von Gioi, P. Monasse, J.-M. Morel, and Z. Tang, "Towards high-precision lens distortion correction," *ICIP*, pp. 4237–4240, 2010.

[14] D. Stevenson and M.M. Fleck, "Nonparametric correction of distortion," Tech. Rep., omp. Sci., U. of Iowa, 1995.

[15] D.C. Brown, "Close-range camera calibration," *Photogrammetric Engieering*, vol. 37, pp. 855–866, 1971.

[16] F. Devernay and O. Faugeras, "Straight lines have to be straight," *Mach. Vision Appli.*, vol. 13, pp. 14–24, 2001.

[17] R. Grompone von Gioi, P. Monasse, J.-M. Morel, and Z. Tang, "Self-consistency and universality of camera lens distortion models," *CMLA Preprint, ENS-Cachan*, 2010.

[18] F. Devernay, "A non-maxima suppression method for edge detection with sub-pixel accuracy," Tech. Rep. 2724, INRIA rapport de recherche, 1995.

[19] R. Grompone von Gioi, J. Jakubowicz, J.-M. Morel, and G. Randall "LSD: A fast line segment detector with a false detection control," *IEEE Trans. on PAMI*, vol. 32, no. 4, pp. 722-732, 2010.